

Effects of Interlayer Interaction on the Superconducting State in YBCO

C. O'Donovan[†] and J. P. Carbotte

Department of Physics & Astronomy, McMaster University, Hamilton, Ontario, Canada L8S 4M1
(October 16, 1996)

For a two layer system in a weak coupling BCS formalism any interlayer interaction, regardless of its sign, enhances the critical temperature. The sign has an effect upon the relative phase of the order parameter in each of the two planes but not upon its magnitude. When one of the planes has a dispersion consistent with CuO chains and no intrinsic pairing interaction there is both an enhancement of the critical temperature and an $s + d$ mixing in both layers as the interlayer interaction is increased. The magnetic penetration depth, c -axis Josephson tunneling, density of states and Knight shift are calculated for several sets of model parameters.

I. INTRODUCTION

The search for the mechanism which causes superconductivity in the copper oxide materials is an ongoing effort which has yet to reach a consensus. One factor which any model should account for is that the critical temperature tends to be higher in systems with multiple adjacent CuO₂ layers; and even in systems, such as YBCO, in which a CuO layer is adjacent to the CuO₂ layers T_c seems to be enhanced.

It is generally believed that the superconducting condensate resides in the CuO₂ planes, although one interpretation of the observed large x - y anisotropy of the zero temperature magnetic penetration depth (a factor of ~ 1.6) in YBCO indicates that there is as much condensate in the CuO chains as in the CuO₂ planes (ie, the condensate in the chains only contributes to the penetration depth for current in the direction parallel to the chains, ie the b -direction). [1] Since it is believed that whatever mechanism is responsible for superconductivity in the copper oxides is intrinsic to the CuO₂ planes some other mechanism for creating superconducting condensate on the CuO chains is required.

In this paper we derive a Hamiltonian for a layered system and, making a simplifying assumption that there is no pairing between electrons which reside in different layers, derive a pair of coupled BCS equations for a system of two layers, each with possibly different dispersion and pairing interactions. In this model Cooper pairs can scatter between the layers so that, as in a two band model, [2] even if there is no pairing interaction in one of the layers there will still be a condensate in that layer due to the interlayer interaction.

Although we make a particular choice for the pairing interaction (which is motivated by the nearly antiferromagnetic Fermi liquid model which leads naturally to a d -wave gap for single CuO₂ planes. [3]) a d -wave solution is also found for other types of non-isotropic pairing interactions. [4] One result of having gap nodes cross the Fermi surface is a low temperature linear behaviour of the magnetic penetration depth, λ_{ii}^{-2} , as is observed in YBCO. [1,5-7] Here we only try to model the low temperature behaviour and relative magnitude [1] in the

x and y directions of the magnetic penetration depth. The $T \sim T_c$ behaviour is only reproduced for values of $2\Delta_{\max}/T_c$ about 1.5 times higher [8] than the value of 4.4 found in the BCS weak coupling approximation. In the two layer model that we study here a higher value of $2\Delta_{\max}/T_c$ is obtained which is closer to that observed in experiments such as ARPES [9] or current-imaging tunneling spectroscopy (CITS) [10] that measure the absolute magnitude of the order parameter.

We find that the presence of the chains destroys the tetragonal symmetry of the CuO₂ planes and shifts the d -wave gap nodes in the CuO₂ plane off the diagonals in agreement with an earlier model. [11] In this case the gap contains an admixture of s - and d -wave symmetry. Calculations of the c -axis Josephson tunneling current show that the positive and negative parts of the order parameter do not cancel, as for d -wave pairing in a tetragonal system, and that the Josephson junction resistance-tunneling current products, $RJ(T = 0)$, are in the range of 0.1-3.0meV, in agreement with the experiments of Sun *et al*, [12]. We also calculate both the normal and superconducting density of states (DOS) for the CuO₂ planes and CuO chains separately since some surface probes, such as CITS, [10] can measure them separately. Finally the Knight shift is calculated separately for both the planes and the chains.

In section II we introduce our Hamiltonian and derive a set of coupled BCS equations for planes and chains and other necessary formulas, particularly the expression for the magnetic penetration depth in this model. In section III we present the the solutions of these BCS equations as well as the results of calculations of the magnetic penetration depth, electronic density of states, c -axis Josephson tunneling, and Knight shift. Section IV contains a short discussion and conclusion.

II. FORMALISM

In this section we will present a Hamiltonian in which multiple layers are coupled through the pairing interactions between adjacent layers. We will then make the assumption that there is no interlayer pairs (ie, that

each Cooper pair resides in only one of the layers) and that there is no single particle interlayer hopping. The Hamiltonian of this special case is then diagonalized and coupled BCS equations derived. We then give expressions for the magnetic penetration depth in this model, the Knight shift, the quasi-particle density of states and the DC Josephson junction resistance-tunneling current product for a c -axis tunnel junction.

The general Hamiltonian is:

$$H = \sum_{\mathbf{k},\alpha\beta} \varepsilon_{\mathbf{k},\alpha\beta} \left(a_{\mathbf{k}\uparrow,\alpha}^\dagger a_{\mathbf{k}\uparrow,\beta} + a_{\mathbf{k}\downarrow,\beta}^\dagger a_{\mathbf{k}\downarrow,\alpha} \right) - \frac{1}{\Omega} \sum_{\mathbf{k},\mathbf{q},\alpha\beta\gamma\delta} V_{\mathbf{k},\mathbf{q},\alpha\beta\gamma\delta} a_{\mathbf{k}\uparrow,\alpha}^\dagger a_{-\mathbf{k}\downarrow,\beta}^\dagger a_{\mathbf{q}\uparrow,\gamma} a_{-\mathbf{q}\downarrow,\delta}, \quad (1)$$

where the greek indices enumerate the layers, the $a_{\mathbf{k},\alpha}^\dagger$ ($a_{\mathbf{k},\alpha}$) create (destroy) electrons of momentum \mathbf{k} in layer α (\mathbf{k} is in units of a^{-1} where a is the lattice parameter), $\varepsilon_{\mathbf{k},\alpha\beta}$ is the electron dispersion, and $V_{\mathbf{k},\mathbf{q},\alpha\beta\gamma\delta}$ is the pairing interaction.

Performing a mean field analysis, we get:

$$H = \sum_{\mathbf{k},\alpha\beta} \varepsilon_{\mathbf{k},\alpha\beta} \left(a_{\mathbf{k}\uparrow,\alpha}^\dagger a_{\mathbf{k}\uparrow,\beta} + a_{\mathbf{k}\downarrow,\beta}^\dagger a_{\mathbf{k}\downarrow,\alpha} \right) - \sum_{\mathbf{k},\alpha\beta} \left(\Delta_{\mathbf{k},\alpha\beta} a_{\mathbf{k}\uparrow,\alpha}^\dagger a_{-\mathbf{k}\downarrow,\beta}^\dagger + \text{H.c.} \right) + C,$$

where C is a constant, H.c. indicates the Hermitian conjugate, $\Delta_{\mathbf{k},\alpha\beta} \equiv \Omega^{-1} \sum_{\mathbf{q},\gamma\delta} V_{\mathbf{k},\mathbf{q},\alpha\beta\gamma\delta} \chi_{\mathbf{q},\gamma\delta}$ are the order parameters and $\chi_{\mathbf{q},\gamma\delta} \equiv \langle a_{\mathbf{q}\uparrow,\gamma} a_{-\mathbf{q}\downarrow,\delta} \rangle$ are the pair susceptibilities.

Writing this in Nambu spinor notation, we get:

$$H = \sum_{\mathbf{k},\alpha\beta} A_{\mathbf{k},\alpha}^\dagger \hat{H}_{\mathbf{k},\alpha\beta} A_{\mathbf{k},\beta}$$

where $A_{\mathbf{k},\alpha}^\dagger \equiv \left[a_{\mathbf{k}\uparrow,\alpha}^\dagger \ a_{-\mathbf{k}\downarrow,\alpha} \right]$ and:

$$\hat{H}_{\mathbf{k},\alpha\beta} \equiv \begin{bmatrix} \varepsilon_{\mathbf{k},\alpha\beta} & \Delta_{\mathbf{k},\alpha\beta} \\ \Delta_{\mathbf{k},\alpha\beta}^\dagger & -\varepsilon_{\mathbf{k},\alpha\beta} \end{bmatrix}. \quad (2)$$

In this model the magnetic penetration depth is given by the expression: [13]

$$\lambda_{ij}^{-2} = \frac{4\pi e^2}{\hbar^2 c^2} \frac{1}{\Omega} \sum_{\mathbf{k},\alpha\beta} \hat{\gamma}_{\mathbf{k},\alpha\beta}^{(i)} \hat{\gamma}_{\mathbf{k},\beta\alpha}^{(j)} \left(\hat{G}_{\mathbf{k},\alpha\beta} |_{\Delta=0} - \hat{G}_{\mathbf{k},\alpha\beta} \right) \quad (3)$$

where:

$$\hat{G}_{\mathbf{k},\alpha\beta} \equiv \frac{\partial f(E_{\mathbf{k},\alpha})}{\partial E_{\mathbf{k},\alpha}} \delta_{\alpha\beta} + \frac{f(E_{\mathbf{k},\alpha}) - f(E_{\mathbf{k},\beta})}{E_{\mathbf{k},\alpha} - E_{\mathbf{k},\beta}} (1 - \delta_{\alpha\beta}),$$

$$\hat{\gamma}_{\mathbf{k},\alpha\beta}^{(i)} \equiv \sum_{\gamma\delta} \hat{U}_{\mathbf{k},\alpha\gamma}^\dagger \frac{\partial \varepsilon_{\mathbf{k},\gamma\delta}}{\partial k_i} \hat{U}_{\mathbf{k},\delta\beta},$$

$\pm E_{\mathbf{k},\alpha}$ are the eigenvalues of Eq. (2), $f(x)$ is the Fermi function, $\delta_{\alpha\beta}$ is a Kronecker delta and $\hat{U}_{\mathbf{k},\alpha\beta}$ is the unitary matrix which diagonalizes Eq. (2). The quantities e , \hbar , and c are the electron charge, Planck's constant and the speed of light respectively.

We now make the following simplification: $V_{\mathbf{k},\mathbf{q},\alpha\gamma} \equiv V_{\mathbf{k},\mathbf{q},\alpha\alpha\gamma\gamma} = V_{\mathbf{k},\mathbf{q},\alpha\beta\gamma\delta} \delta_{\alpha\beta} \delta_{\gamma\delta}$ and $\varepsilon_{\mathbf{k},\alpha} \equiv \varepsilon_{\mathbf{k},\alpha\alpha} = \varepsilon_{\mathbf{k},\alpha\beta} \delta_{\alpha\beta}$. This means that there is only intralayer pairing and no interlayer pairing (ie, $\Delta_{\mathbf{k},\alpha} \equiv \Delta_{\mathbf{k},\alpha\beta} \delta_{\alpha\beta}$ and $\chi_{\mathbf{q},\gamma} \equiv \chi_{\mathbf{q},\gamma\delta} \delta_{\alpha\beta}$ are both diagonal in the greek indices) and there is no single particle interlayer hopping. This Hamiltonian has the same form as that for a two band model studied by one of us [3] in an earlier publication and is similar to that studied by others. [14–16] Interlayer pairing [16–18] has also been studied.

The Hamiltonian has eigenvalues given by $E_{\mathbf{k},\alpha} = \pm \sqrt{\varepsilon_{\mathbf{k},\alpha}^2 + \Delta_{\mathbf{k},\alpha}^2}$ and is diagonalized by the unitary matrix:

$$\hat{U}_{\mathbf{k},\alpha} = \begin{bmatrix} u_{\mathbf{k},\alpha} & v_{\mathbf{k},\alpha} \\ -v_{\mathbf{k},\alpha} & u_{\mathbf{k},\alpha} \end{bmatrix}, \quad (4)$$

where:

$$u_{\mathbf{k},\alpha} \equiv \sqrt{\frac{1}{2} \left(1 + \frac{\varepsilon_{\mathbf{k},\alpha}}{E_{\mathbf{k},\alpha}} \right)}$$

$$v_{\mathbf{k},\alpha} \equiv \sqrt{\frac{1}{2} \left(1 - \frac{\varepsilon_{\mathbf{k},\alpha}}{E_{\mathbf{k},\alpha}} \right)}$$

are the usual BCS coherence factors. Using this unitary transformation (4) we can evaluate the pair susceptibilities to get:

$$\chi_{\mathbf{q},\alpha} \equiv \langle a_{\mathbf{q}\uparrow,\alpha} a_{-\mathbf{q}\downarrow,\alpha} \rangle = \frac{\Delta_{\mathbf{q},\alpha}}{2E_{\mathbf{q},\alpha}} \tanh \left(\frac{E_{\mathbf{q},\alpha}}{2k_B T} \right), \quad (5)$$

where T is the temperature and k_B is Boltzmann's constant. Note that if we had included the interlayer pairing from Eq. 1 we would have susceptibilities of the form $\langle a_{\mathbf{q}\uparrow,\alpha} a_{-\mathbf{q}\downarrow,\beta} \rangle$ with $\alpha \neq \beta$ and both the eigenvalues and the unitary matrix (4) would be much more complicated.

For a bilayer system (ie, $\alpha = 1, 2$) the BCS equations are:

$$\Delta_{\mathbf{k},1} = \frac{1}{\Omega} \sum_{\mathbf{q}} (V_{\mathbf{k},\mathbf{q},11} \chi_{\mathbf{q},1} + V_{\mathbf{k},\mathbf{q},12} \chi_{\mathbf{q},2})$$

$$\Delta_{\mathbf{k},2} = \frac{1}{\Omega} \sum_{\mathbf{q}} (V_{\mathbf{k},\mathbf{q},12} \chi_{\mathbf{q},1} + V_{\mathbf{k},\mathbf{q},22} \chi_{\mathbf{q},2}), \quad (6)$$

where we have taken $V_{\mathbf{k},\mathbf{q},12} = V_{\mathbf{k},\mathbf{q},21}$, although in general only $V_{\mathbf{k},\mathbf{q},12} = V_{\mathbf{k},\mathbf{q},21}^\dagger$ is required.

Noting that $\chi_{\mathbf{q},2}$ changes sign (see Eq. 5) with $\Delta_{\mathbf{k},2}$ we see that this set of equations (6) is unchanged by the substitution $\{\Delta_{\mathbf{k},2}, V_{\mathbf{k},\mathbf{q},12}\} \rightarrow \{-\Delta_{\mathbf{k},2}, -V_{\mathbf{k},\mathbf{q},12}\}$ which

means that the overall sign of $V_{\mathbf{k},\mathbf{q},12}$ only affects the relative sign of the order parameters in the two layers and not their magnitudes. This is interesting because it means that the effect on T_c of having an interlayer interaction is independent of whether this interaction is attractive or repulsive, although some calculated properties (eg, c -axis Josephson tunneling current) still depend upon the relative sign of the interlayer interaction. *It is important to emphasize that any interlayer interaction, either attractive or repulsive, tends to enhance T_c and that this is consistent with the observation that T_c is higher in materials with multiple adjacent CuO layers.* This well known result can be easily shown by examining the coupled BCS equations (6) near $T \sim T_c$. In this limit we can write:

$$\begin{aligned}\Delta_{\mathbf{k},\alpha} &= \Delta_\alpha \eta_{\mathbf{k}} \\ V_{\mathbf{k},\mathbf{q},\alpha\beta} &= V_{\alpha\beta} \eta_{\mathbf{k}} \eta_{\mathbf{q}}\end{aligned}$$

where Δ_α and $V_{\alpha\beta}$ are numbers and $\eta_{\mathbf{k}}$ is a normalized function which could be taken to be d -wave and corresponds to the highest T_c . The coupled BCS equations (6) can then be written as:

$$\begin{aligned}\Delta_1 &= \Delta_1 V_{11} \frac{1}{\Omega} \sum_{\mathbf{q}} \frac{(\eta_{\mathbf{q}})^2}{\varepsilon_{\mathbf{q},1}} \tanh\left(\frac{\varepsilon_{\mathbf{q},1}}{2k_B T_c}\right) \\ &+ \Delta_2 V_{12} \frac{1}{\Omega} \sum_{\mathbf{q}} \frac{(\eta_{\mathbf{q}})^2}{\varepsilon_{\mathbf{q},2}} \tanh\left(\frac{\varepsilon_{\mathbf{q},2}}{2k_B T_c}\right)\end{aligned}\quad (7a)$$

$$\begin{aligned}\Delta_2 &= \Delta_1 V_{12} \frac{1}{\Omega} \sum_{\mathbf{q}} \frac{(\eta_{\mathbf{q}})^2}{\varepsilon_{\mathbf{q},1}} \tanh\left(\frac{\varepsilon_{\mathbf{q},1}}{2k_B T_c}\right) \\ &+ \Delta_2 V_{22} \frac{1}{\Omega} \sum_{\mathbf{q}} \frac{(\eta_{\mathbf{q}})^2}{\varepsilon_{\mathbf{q},2}} \tanh\left(\frac{\varepsilon_{\mathbf{q},2}}{2k_B T_c}\right).\end{aligned}\quad (7b)$$

We now assume that Δ_1 is the dominant superconducting channel when $V_{12} = V_{21} = 0$ and obtain assuming an infinite band with cutoff ω_C :

$$\Delta_1 = (\Delta_1 \lambda_{11} + \Delta_2 \lambda_{12}) \ln\left(\frac{1.13\omega_C}{T_c}\right)\quad (8a)$$

$$\Delta_2 = (\Delta_1 \lambda_{21} + \Delta_2 \lambda_{22}) \ln\left(\frac{1.13\omega_C}{T_c}\right),\quad (8b)$$

where $\lambda_{ij} \equiv V_{ij} \times$ the density of electronic states at the Fermi surface. Substitution of equation (8b) into (8a) leads to a quadratic in $\ln(1.13\omega_C/T_c)$ with solution:

$$T_c = 1.13e^{1/\tilde{\lambda}}\quad (9)$$

with:

$$\tilde{\lambda} = \frac{1}{2} \left[\lambda_{11} + \lambda_{22} + \sqrt{(\lambda_{11} - \lambda_{22})^2 + 4\lambda_{12}\lambda_{21}} \right].\quad (10)$$

This result is well known and is given by equation (6.3) on page 105 of Mechanisms of Conventional and High T_c Superconductivity. [23] It is also found as equation (40)

of H. Chi and Carbotte. [3] We note that λ_{12} , whatever its sign, increases $\tilde{\lambda}$ and so increases T_c .

If we had taken $V_{\mathbf{k},\mathbf{q},12}$ as complex the symmetry would be $\{\Delta_{\mathbf{k},2}, V_{\mathbf{k},\mathbf{q},12}\} \rightarrow \{\Delta_{\mathbf{k},2} e^{-i\phi}, V_{\mathbf{k},\mathbf{q},12} e^{i\phi}\}$ where $V_{\mathbf{k},\mathbf{q},12} = |V_{\mathbf{k},\mathbf{q},12}| e^{i\phi}$, and the relative phase between the layers would no longer be ± 1 .

We note that by performing the unitary transformation $\hat{S}^\dagger \hat{H} \hat{S}$ where:

$$\hat{S} \equiv \frac{1}{\sqrt{2}} \begin{bmatrix} 1 & 1 & 0 & 0 \\ 1 & -1 & 0 & 0 \\ 0 & 0 & 1 & 1 \\ 0 & 0 & 1 & -1 \end{bmatrix},$$

and making the substitutions $V_{11} = V_{22} = V_{\parallel} + V_{\perp}$, $V_{12} = V_{\parallel} - V_{\perp}$, $\varepsilon_1 = \varepsilon + t$ and $\varepsilon_2 = \varepsilon - t$ we obtain both the Hamiltonian and BCS equations used by Liu *et al.* [19] Our work differs from theirs in that we allow both the dispersion and the interaction to be different in the two layers. This is important not only because we are able to model systems such as YBCO in which there are CuO₂ planes and CuO chains, but also because the order parameter in each of the layers may differ in sign even in two identical layers. [16] Other workers have studied models in which the electrons in the pairs reside in different layers [17] (ie, in which only $\chi_{\mathbf{k},12}$ is non-zero) as well as models in which there is no intralayer interaction [16,18] (ie, in which only $V_{\mathbf{k},\mathbf{q},12}$ is non-zero).

After solving the set of coupled BCS equations (6) at $T = 0$ using a FFT technique [4,11,20] we approximate the order parameters, $\Delta_{\mathbf{k},1}$ and $\Delta_{\mathbf{k},2}$, with:

$$\begin{aligned}\Delta_{\mathbf{k},\alpha} &= \left(\Delta_\alpha^{(s_o)} \eta_{\mathbf{k}}^{(s_o)} + \Delta_\alpha^{(s_x)} \eta_{\mathbf{k}}^{(s_x)} + \Delta_\alpha^{(d)} \eta_{\mathbf{k}}^{(d)} \right) \\ &\times \tanh\left(1.74\sqrt{T_c/T-1}\right),\end{aligned}\quad (11)$$

where the $\eta_{\mathbf{k}}^{(\cdot)}$ are the three lowest harmonics given by:

$$\begin{aligned}\eta_{\mathbf{k}}^{(s_o)} &= 1 \\ \eta_{\mathbf{k}}^{(s_x)} &= \cos(k_x) + \cos(k_y) \\ \eta_{\mathbf{k}}^{(d)} &= \cos(k_x) - \cos(k_y),\end{aligned}$$

and the $\Delta_\alpha^{(\cdot)}$ are their amplitudes. The amplitudes of the higher harmonics are all very much smaller in magnitude and the gap nodes and the maximum magnitude of the gap, which are the most important features of the order parameter, are essentially unchanged by this approximation. We also calculate the magnetic penetration depth which in this system, since the $\hat{\gamma}_{\mathbf{k},\alpha\beta}^{(i)}$ are diagonal in the greek indices, is given by the simplified expression:

$$\begin{aligned}\lambda_{ij}^{-2} &= \frac{4\pi e^2}{\hbar^2 c^2} \frac{1}{\Omega} \sum_{\mathbf{k},\alpha} \frac{\partial \varepsilon_{\mathbf{k},\alpha}}{\partial k_i} \frac{\partial \varepsilon_{\mathbf{k},\alpha}}{\partial k_j} \\ &\times \left(\frac{\partial f(\varepsilon_{\mathbf{k},\alpha})}{\partial \varepsilon_{\mathbf{k},\alpha}} - \frac{\partial f(E_{\mathbf{k},\alpha})}{\partial E_{\mathbf{k},\alpha}} \right)\end{aligned}\quad (12)$$

which is the usual expression [20] summed over the layers.

The curvature of the penetration depth curve, $\lambda_{ii}^{-2}(T)$, (and also its low temperature slope) is governed by the ratio $2\Delta_{\max}/T_c$, where Δ_{\max} is the maximum value of the order parameter in the first Brillouin zone, and is close to a straight line for the d -wave BCS value of $2\Delta_{\max}/T_c = 4.4$. The presence of the interlayer interaction increases this ratio and makes the $\lambda_{ii}^{-2}(T)$ curve have a downward curvature. Experimental measurements of both the ratio $2\Delta_{\max}/T_c$ [10,21] as well as the penetration depth in high quality crystals of both YBCO [1] and BSCO [22] indicate that this ratio is quite high in the HTC materials – on the order of 6 or 7.

Other quantities calculated are the Knight shift which is given by:

$$K(T) \propto \frac{1}{\Omega} \sum_{\mathbf{k}} \frac{\partial f(E_{\mathbf{k}})}{\partial E_{\mathbf{k}}}, \quad (13)$$

the normal state electronic DOS which is given by:

$$\begin{aligned} N(\omega) &= \frac{1}{\Omega} \sum_{\mathbf{k}} \delta(\varepsilon_{\mathbf{k}} - \omega) \\ &= \lim_{\Gamma \rightarrow 0} \frac{1}{\pi\Omega} \sum_{\mathbf{k}} \frac{\Gamma}{(\varepsilon_{\mathbf{k}} - \omega)^2 + \Gamma^2}, \end{aligned} \quad (14)$$

the superconducting electronic DOS which is given by:

$$\begin{aligned} N(\omega) &= \frac{1}{\Omega} \sum_{\mathbf{k}} \delta(E_{\mathbf{k}} - \omega) \\ &= \lim_{\Gamma \rightarrow 0} \frac{1}{\pi\Omega} \sum_{\mathbf{k}} \frac{\Gamma}{(E_{\mathbf{k}} - \omega)^2 + \Gamma^2}, \end{aligned} \quad (15)$$

and the c -axis Josephson junction resistance-tunneling current product, $RJ(T)$, through a superconductor-insulator-superconductor junction for incoherent c -axis tunneling is given by the relation [24]:

$$RJ(T) = \frac{2\pi T}{N^L(0)N^R(0)\pi^2} \sum_n A^L(\omega_n)A^R(\omega_n), \quad (16)$$

where:

$$A^{L(R)}(\omega_n) \equiv \frac{1}{\Omega} \sum_{\mathbf{k}} \frac{\Delta_{\mathbf{k}}^{L(R)}}{(\varepsilon_{\mathbf{k}}^{L(R)})^2 + (\Delta_{\mathbf{k}}^{L(R)})^2 + (\omega_n)^2}.$$

in which the superscript L(R) indicates on which side of the junction the dispersion and order parameter are on, the sum over $\omega_n \equiv \pi T(2n - 1)$ is for all Matsubara frequencies, R is the resistance of the junction and $N^{L(R)}(0)$ is the normal state electronic DOS given by equation (14). If the tunneling were coherent the matrix element (which is incorporated into R) would have a $(\mathbf{k} - \mathbf{k}')$ dependence, and the sums over \mathbf{k} -space wouldn't be separable.

III. RESULTS

In this section we make an explicit choice for the dispersions and interactions and then present the results of our numerical solutions to the coupled BCS equations (6) as well as the results of our calculations of the magnetic penetration depth, densities of states, Knight shift and Josephson current. As we wish to model YBCO we will want to account for both the CuO_2 planes as well as the CuO chains. Further, we will assume that we do not have a pairing interaction in the chains, but only in the planes as well as an interlayer interaction. This means that all of the order parameter in the chains is due to the interlayer interaction. We note that although our solution technique [4] allows the order parameters to be complex and to have a relative phase between layers we find that in the models studied here, to within an overall phase, the order parameters are all real with a relative phase of ± 1 .

For the dispersions, $\varepsilon_{\mathbf{k},\alpha}$, we use:

$$\begin{aligned} \varepsilon_{\mathbf{k},\alpha} &= -2t_{\alpha} [(1 + \epsilon_{\alpha}) \cos(k_x) + \cos(k_y) \\ &\quad - 2B_{\alpha} \cos(k_x) \cos(k_y) - (2 - 2B_{\alpha} - \mu_{\alpha})], \end{aligned} \quad (17)$$

where the parameters $\{t_{\alpha}, \epsilon_{\alpha}, B_{\alpha}, \mu_{\alpha}\}$ are chosen so that the Fermi surface and bandwidth are close approximations to those observed experimentally [25] (see Fig. 1). In order to model YBCO we chose $\{100, 0, 0.45, 0.51\}$ for the planes and $\{-50, -0.9, 0, 1.2\}$ for the chains. In both dispersions t_{α} , which sets the overall energy scale, is in units of meV. For the interactions, $V_{\mathbf{k},\mathbf{q},\alpha\beta}$, we chose an MMP form: [2]

$$V_{\mathbf{k},\mathbf{q},\alpha\beta} = g_{\alpha\beta} \frac{-\chi_{\circ}}{1 + \xi_{\circ}^2 |\mathbf{k} - \mathbf{q} - \mathbf{Q}|^2},$$

where χ_{\circ} is a constant that sets the scale of the susceptibility, ξ_{\circ} is the magnetic coherence length, $\mathbf{Q} \equiv (\pi, \pi)$ is the commensurate nesting vector, and $g_{\alpha\beta}$ is the coupling to the conduction electrons, the size of which can be fixed to get a desired value of the critical temperature and can be considered to contain χ_{\circ} . The remaining parameter, ξ_{\circ} , is given in reference [2] and will not be varied in this work. In this paper we set $g_{22} = 0$ ie, there is no intrinsic pairing in the chains. This means that any superconductivity in the chains is induced by the interlayer interaction, g_{12} , since we have set the hopping between layers to zero. The effect of an interlayer hopping has been extensively studied in works by Atkinson and Carbotte [13] as well as others. [14,15,17–19]

We solve the coupled BCS equations (6) using a FFT technique. [4] In Fig. 2 we plot the lowest three Fourier components (11) of the zero temperature order parameter as a function of the interlayer interaction (higher Fourier components are all much smaller in magnitude) for two different intralayer interactions (upper and lower frames) in the planes (left frames) and chains (right frames). The values plotted in Fig. 2 are the amplitudes $\Delta_{\alpha}^{(s_{\circ})}$, $\Delta_{\alpha}^{(s_x)}$

and $\Delta_\alpha^{(d)}$ given by (11) with $\alpha = 1$ for the plane layers (right frames) and $\alpha = 2$ for the chain layers (left frames). For the orthorhombic system studied here all three of these harmonics belong to the same irreducible representation of the crystal point group except for $g_{12} = 0$ when the tetragonal CuO_2 layer is decoupled from the orthorhombic CuO layer. Recent CITS measurements [26] show that the gap has a magnitude of $\sim 20\text{meV}$ in the chains and $\sim 30\text{meV}$ in the planes which would indicate that g_{12} is large.

For the first choice of intralayer interaction (upper frames), $g_{11} = 26.2$, and there is no order parameter in the chains when there is no interlayer interaction (ie, $g_{12} = 0$) and the order parameter in the planes is pure d -wave. As the interlayer interaction is increased from zero, s -wave components appear in the planes and all three components appear in the chains. This “ $s + d$ mixing” is caused by the breaking of the tetragonal symmetry upon the introduction of the chains; there is no relative phase between the s - and d -wave components within either the planes or chains but there can be a relative phase between the order parameter in the planes and chains. In the range of g_{12} explored here the d -wave component in the plane remains dominant but for sufficiently strong interlayer interaction the isotropic s -wave component eventually dominates [27] (ie, the gap nodes disappear). For interaction parameters $\{g_{11}, g_{12}, g_{22}\} = \{26.2, 10, 0\}$ the critical temperature is 100K and the maximum value of the gap in the Brillouin zone is 27.5meV in the planes and 8.0meV in the chains, while the maximum values on the Fermi surfaces are approximately 22meV and 7meV respectively. The ratio $2\Delta_{\text{max}}/T_c$ is 6.4 in the planes and 1.9 in the chains.

For the second choice of intralayer interaction (lower frames), $g_{11} = 9.18$, there is no order parameter in either the chains or the planes when there is no interlayer interaction (ie, $g_{12} = 0$). As the interlayer interaction is increased d -wave and then s -wave components of the order parameter appear in both the planes and chains. Again, there is no relative phase between the s - and d -wave components within either the planes or chains but there can be a relative phase between the order parameter in the planes and chains. In the range of g_{12} explored here, the d -wave component is dominant. At approximately $g_{12} = 15$ the gap nodes no longer cross the Fermi surface in the chains; the feature at $g_{12} \sim 25$ coincides with the gap nodes leaving the Brillouin zone and isotropic s -wave becoming dominant. For interaction parameters $\{g_{11}, g_{12}, g_{22}\} = \{9.18, 20, 0\}$ the critical temperature is again 100K and the maximum value of the gap in the Brillouin zone is now 32.8meV in the planes and 20.1meV in the chains, while the maximum values on the Fermi surfaces are approximately 27meV and 17meV respectively. The ratio $2\Delta_{\text{max}}/T_c$ is 7.6 in the planes and 4.7 in the chains.

Note that for $g_{12} > 0$ all of the s -wave components of the order parameters in both the planes and chains have

the same relative sign and the d -wave components have opposite signs, while for $g_{12} < 0$ all of the relative signs are reversed but that the magnitudes of the components are insensitive to the sign of g_{12} as noted after Eq. 6.

In Fig. 3 we plot the density of states (DOS) for the planes (left frames) and chains (right frames) calculated using the lowest three harmonics (11) of the solution to the BCS equations (6) with two sets of interaction parameters. The dotted curves are the normal state DOS (NSDOS) and the solid curves are the superconducting DOS (SCDOS). The insets show the Fermi surface (dashed curves) and gap nodes (solid curves) in the first Brillouin zone (with (π, π) at the center). The peak in the NSDOS (dotted curves) is the van Hove singularity located at $2t_\alpha(2 - \mu_\alpha - 4B_\alpha \pm \epsilon_\alpha)$ which is at -62meV in the plane layers (left frames) and at 10 and -170meV in the chain layers (right frames). They are caused by the saddle points in the electron dispersions, $\epsilon_{\mathbf{k}, \alpha}$, at $(0, \pm\pi)$ and $(\pm\pi, 0)$. These van Hove singularities are shifted by the presence of the superconducting order parameter (solid curves) by an amount that depends upon the value of the order parameter at the saddle points; [28] in frame (c) these values are very different and the van Hove singularity is split, in frame (a) these values are almost the same and no splitting is evident.

An interesting feature is that the low energy behaviour ($\omega \sim 0$) of the SCDOS is governed by the *smallest* local *maxima* of the gap on the Fermi surface when the gap nodes cross the Fermi surface and by the *minima* of the gap on the Fermi surface when there is no gap nodes which cross the Fermi surface. In Fig. 4 the magnitude of the gap along the Fermi surface is plotted. In Fig. 4a-c one can see that there are two different local maxima of the gap on the Fermi surface and these maxima are (to first order [28]) manifested as twin peaks in the SCDOS (Fig. 3a-c); these peaks are distinct from the van Hove singularities which are also present in the normal DOS (dotted curves in Fig. 3) and which are slightly shifted in the superconducting state. [28] In frame (a) of Fig. 4 the local maxima of the gap on the Fermi surface are 16 and 18meV; in (b) they are 1 and 7meV, and in (c) they are 25 and 3meV. In (d) one can see that there are no gap nodes which cross the Fermi surface; the maximum and minimum value of the gap on the Fermi surface are 17 and 4meV respectively. In Fig. 3d the finite gap in the SCDOS corresponds to the minimum of the gap on the Fermi surface and the peak to the maximum.

The Josephson junction resistance-tunneling current product, $RJ(T = 0)$, for a c -axis YBCO-Pb junction, given by (16) with $\Delta_{\mathbf{k}}^L$ and $\epsilon_{\mathbf{k}}^L$ appropriate for Pb, [11] are $\pm 0.25\text{meV}$ and $\pm 2.2\text{meV}$ for the planes and 2.2meV and 3.4meV for the chains for the two choices of $g_{\alpha\beta}$ made, in agreement with earlier calculations. [11] The relative sign is due to the relative sign of the s -wave components (ie, the only part which contributes) of the order parameters. The actual c -axis Josephson junction resistance-tunneling current product, $RJ(T)$, for a junction made with untwinned YBCO would be some weighted average

of the plane and chain c -axis tunneling currents depending upon the relative abundance of chains and planes in the top layer of the YBCO. For a twinned sample with both twins equally abundant there would be zero net tunneling current, although there is evidence that for single crystals of YBCO there can be up to a 5:1 ratio in the relative abundance of the two twin orientations. [29] We note that due to the different magnitudes of the order parameters in the two layers the model presented here is consistent with the observed π shifts in corner junctions [30–33] for both attractive and repulsive interlayer interactions, g_{12} .

In Fig. 5 we have plotted the magnetic penetration depth (left frames) and the Knight shift (right frames) calculated with the lowest three harmonics (11) of the solutions of the BCS equations (6) for the two choices of interaction parameters. In the penetration depth frames (left) the solid curve is for the x -direction (along the chains) and the dashed curve is for the y -direction (perpendicular to the chains). The dotted curve is $1 - (T/T_c)^2$ and is plotted for comparison. The ratio $\lambda_{yy}/\lambda_{xx}$ at zero temperature is 1.37 for both interaction parameter choices since the zero temperature penetration depth is a normal state property (ie, the second term in Eq. 12 does not contribute at zero temperature). The zero temperature penetration depth is largely governed by the bandwidth (ie, $4t_\alpha(2 - \epsilon_\alpha)$) – the larger the bandwidth the larger the zero temperature penetration depth.

As pointed out above, the curvature of the penetration depth curve, $\lambda_{ii}^{-2}(T)$, is largely governed by the ratio $2\Delta_{\max}/T_c$ and is a straight line for the d -wave BCS value of 4.4. The presence of the chain layer and the interlayer interaction increases this ratio in the plane layer but it remains low in the chain layer due to the absence of an interaction in this layer. It is this lower value that makes $\lambda_{yy}^{-2}(T)$ (along the chains) have upward curvature (solid curves).

One can see (Fig. 5a,c) that the in-plane penetration depth perpendicular to the chains (dashed curve) closely resembles that observed experimentally in high quality crystals, [1,22] and is largely determined by the presence of gap nodes crossing the Fermi surface, which cause the low temperature linear behaviour, and the ratio $2\Delta_{\max}/T_c$ which, for values above ~ 4.4 , make the curve of $\lambda_{ii}^{-2}(T)$ have downward curvature. The penetration depth along the chains (solid curves), however, has an overall upward curvature due to the low values of $2\Delta_{\max}/T_c$ in the chains. It is the component of the penetration depth due to the chains that makes the overall $\lambda_{yy}^{-2}(T)$ have downward curvature. The component of the penetration depth due to the chains perpendicular to the chains does not contribute significantly to the overall penetration depth in this direction, λ_{yy}^{-2} , is due almost entirely to the CuO₂ layers. For a single plane model [20] we would have $\{g_{11}, g_{12}, g_{22}\} = \{30, 0, 0\}$, $2\Delta_{\max}/T_c$ would be 4.5, and the penetration depth would closely resemble the straight line $1 - (T/T_c)$. [20]

The Knight shift (Fig. 5b,d), which is calculated in-

dependently for the planes (solid curves) and chains (dashed curves), has a low temperature power law behaviour when the gap nodes cross the Fermi surface (planes, both figures and chains in upper figure) and an exponential behaviour when the gap is finite over all the Fermi surface (chains, lower figure). When these quantities are measured [8] the distinction between a power law and exponential behaviour rests upon the choice zero and so is not a reliable indicator of the presence of gap nodes on the Fermi surface.

IV. CONCLUSION AND DISCUSSION

We have derived a general expression for the Hamiltonian in a multi-layer system and then made a simplification and have explicitly diagonalized the Hamiltonian. A set of two coupled BCS equations are then derived for this simplified system which is subsequently solved numerically by a FFT technique. This technique, unlike others, [18,16] makes no assumptions about the functional form (and hence the symmetry) of the order parameter in either layer nor any relationship between the order parameters in the different layers.

Using the three lowest harmonics (11) of the solutions found for the coupled BCS equations (6) the magnetic penetration depth (12), normal and superconducting density of states (14,15), Knight shift (13) and c -axis Josephson resistance-tunneling current products (16) were calculated.

Our choice of electron dispersion relations were made so as to approximate the YBCO system in which there are layers consisting of CuO₂ planes as well as layers which contain CuO chains. Our choice of interactions was made so that there is a pairing interaction in the CuO₂ layer as well as an interlayer interaction, but no pairing interaction in the CuO layer.

The solution of the BCS equations is predominately of a d -wave character, but because the tetragonal symmetry is broken by the presence of the chains there is some mixture of s -wave order parameter with no relative phase between the components, although the relative sign of the order parameter in the planes and chains may be ± 1 . Further, we find that due to a symmetry in the set of coupled BCS equations derived, the sign of the interlayer interaction affects only the relative sign of the order parameter in the two layers and not their absolute magnitudes (although some properties could be affected by this relative sign). We also find that any interlayer interaction strongly enhances the zero temperature order parameter, and hence the critical temperature. This is consistent with the observation that T_c is higher in materials with multiple adjacent CuO₂ layers.

Furthermore, we find that the presence of gap nodes in only one of the layers is enough to produce a low temperature linear behaviour for the penetration depth, although if the minimum gap in the chains is too large the

$\lambda_{xx}^{-2}(T)$ and $\lambda_{yy}^{-2}(T)$ curves can cross. Our calculation of the magnetic penetration depth gives a form that is similar to that measured experimentally perpendicular to the chains, but not along the chains due to the small value of $2\Delta_{\max}/T_c$ in the chains. This leads us to speculate that there may be intrinsic pairing in the CuO chains of the same order as in the CuO₂ planes since the $2\Delta_{\max}/T_c$ ratios must both be large (6 to 7) for the low temperature slope of the $\lambda_{ii}^{-2}(T)$ curves to be approximately equal as is observed in experiments. [1,22] This would tend to support the simple single band orthorhombic model previously proposed by us. [11,20]

Our calculation of the superconducting density of states indicate that a surface probe may measure very different results depending upon whether the top layer is CuO chains or CuO₂ planes. Depending upon the interlayer pairing strength the CuO chain layer may have a very narrow “*d*-wave” type gap or a finite “isotropic *s*-wave” type gap.

Our calculation of the *c*-axis Josephson resistance-tunneling current products, $RJ(T=0)$, for a YBCO-Pb junction for several choices of $g_{\alpha\beta}$ range from 0.18meV to 0.50meV for the planes and 2.35meV to 3.06meV for the chains, with possibly a relative sign between the chain and plane layers due to the relative sign of the *s*-wave components of the order parameters. The actual *c*-axis Josephson resistance-tunneling current product for a junction made with untwinned YBCO would be some weighted average of the plane and chain results depending upon the relative abundance of chains and planes in the top layer of the YBCO. For a twinned sample with both twins equally abundant there would be zero net tunneling current although there is evidence that for single crystals of YBCO there can have up to a 5:1 ratio in the relative abundance of the two twin orientations. [29]

ACKNOWLEDGEMENTS

Research supported in part by the Natural Sciences and Engineering Research Council of Canada (NSERC) and by the Canadian Institute for Advanced Research (CIAR). We would like to thank W. A. Atkinson and A. M. Westgate for discussions and insights.

[†] Electronic address: odonovan@mcmaster.ca

- [1] D.N. Basov, R. Liang, D.A. Bonn, W.N. Hardy, B. Dabrowski, M. Quijada, D.B. Tanner, J.P. Rice, D.M. Ginsberg and T. Timusk Phys. Rev. Lett. **74**, 598 (1995).
- [2] A.J. Millis, H. Monien and D. Pines, Phys. Rev. **B 42**, 167 (1990).
- [3] H. Chi and J.P. Carbotte, Physics **C 169**, 55 (1990).
- [4] C. O’Donovan and J.P. Carbotte, Physica **C 252** 87 (1995).
- [5] D.A. Bonn, P. Dosanjh, R. Liang and W.N. Hardy, Phys. Rev. Lett. **68**, 2390 (1992).
- [6] W.N. Hardy *et al*, Phys. Rev. Lett. **70**, 3999 (1993).
- [7] D.A. Bonn, S. Kamal, K. Zhang, R. Liang, D.J. Baar, E. Kleit and W.N. Hardy, Phys. Rev. **B 50**, 4051 (1994).
- [8] N. Bulut and D.J. Scalapino, Phys. Rev. **B 45**, 2371 (1992).
- [9] H. Ding, J.C. Campuzano *et al.*, Phys. Rev. Lett. **50**, 1333 (1994).
- [10] H.L. Edwards, J.T. Markert, and A.L. de Lozanne, Phys. Rev. Lett. **69**, 2967 (1992).
- [11] C. O’Donovan, D. Branch, J.P. Carbotte and J. Preston, Phys. Rev. **B 51**, 6588 (1995).
- [12] A.G. Sun *et al.*, Phys. Rev. Lett. **72**, 2267 (1994).
- [13] W.A. Atkinson and J.P. Carbotte, Phys. Rev. **B 52**, 10601 (1995).
- [14] R.A. Klemm and S.H. Liu, Physics **C 191**, 383 (1992).
- [15] S.H. Liu and R.A. Klemm, Phys. Rev. **B 45**, 415 (1992).
- [16] R. Combescot and X. Leyranas, Phys. Rev. Lett. **75**, 3732 (1995).
- [17] S. Kettemann and K.B. Efetov, Phys. Rev. **B 46**, 8515 (1992).
- [18] T. Xiang and J.M. Wheatley, Phys. Rev. Lett. **76** 134 (1996).
- [19] D.Z. Liu, K. Levin and J. Maly, Phys. Rev. **B 51**, 8680 (1995).
- [20] C. O’Donovan and J.P. Carbotte, Phys. Rev. **B 52**, 4548 (1995).
- [21] I. Maggio-Aprile, Ch. Renner, A. Erb, E. Walker and O. Fisher, Phys. Rev. Lett. **75** 2754 (1995).
- [22] T. Jacobs, S. Sridhar, Qiang Li, G.D. Gu and N. Koshizuka, Phys. Rev. Lett. **75**, 4516 (1995).
- [23] Mechanisms of Conventional and High T_c Superconductivity, V.Z. Kresin, H. Morawitz and S.A. Wolf, Oxford University Press (1993).
- [24] V. Ambegaokar and A. Baratoff, Phys. Rev. Lett. **10**, 486 (1963); **11**, 104 (1964).
- [25] K. Gofron, J.C. Campuzano, A.A. Abrikosov, M. Lindroos, A. Bansil, H. Ding, D. Koelling, and B. Dabrowski, Phys. Rev. Lett. **73**, 3302 (1994).
- [26] H.L. Edwards, D.J. Derro, A.L. Barr, J.T. Markert, and A.L. de Lozanne, Phys. Rev. Lett. **75**, 1387 (1992).
- [27] A.I. Liechtenstein, I.I. Mazin and O.K. Anderson, Phys. Rev. Lett. **74**, 2303 (1995).
- [28] C. Zhou and H.J. Schulz, Phys. Rev. **B 45**, 7397 (1992).
- [29] B. Gaulin, private communication.
- [30] D.A. Wollman, D.J. Van Harlingen, W.C. Lee, D.M. Ginsberg and A.J. Leggett, Phys. Rev. Lett. **71**, 2134 (1993).
- [31] D.A. Brawner and H.R. Ott, Phys. Rev. **B 50**, 6530 (1994).
- [32] C.C. Tsuei *et al.*, Phys. Rev. Lett. **73**, 593 (1994).
- [33] A. Mathai, Y. Gim, R.C. Black, A. Amar and F.C. Wellstood, Phys. Rev. Lett. **74**, 4523 (1995).

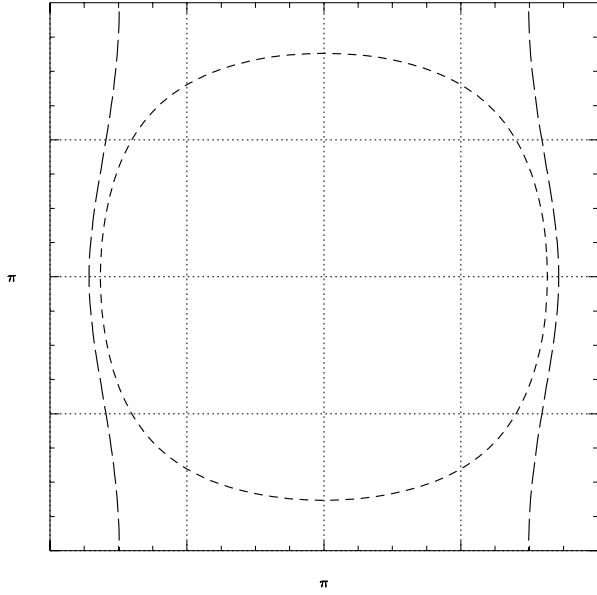


FIG. 1. Model of YBCO Fermi surfaces for chains (long dashed curve) and planes (closed short dashed curve) in the first Brillouin zone. The (π, π) point is at the center of the figure. For the chains the parameters $\{t_\alpha, \epsilon_\alpha, B_\alpha, \mu_\alpha\}$ in Eq. 17 are $\{-50, -0.9, 0, 1.2\}$ and for the planes they are $\{100, 0, 0.45, 0.51\}$.

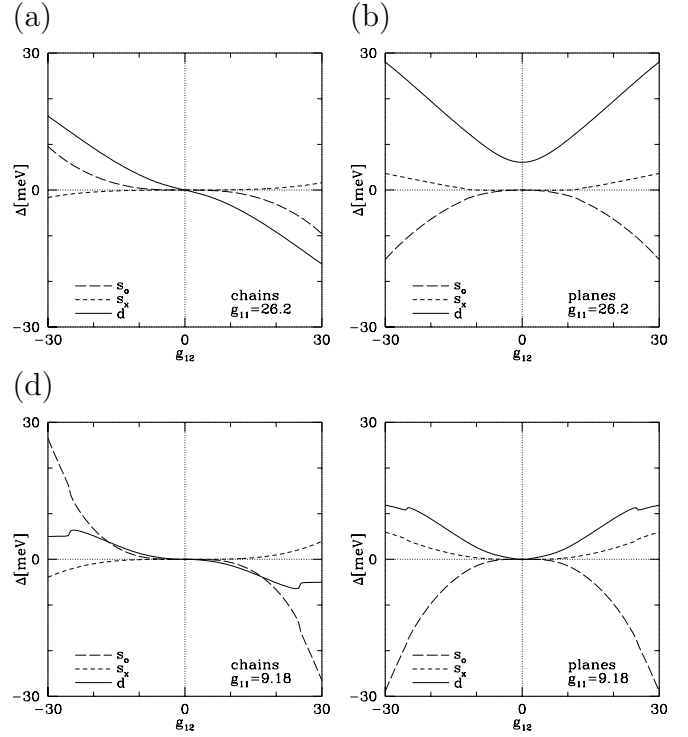


FIG. 2. Calculation of the zero temperature order parameters as a function of the interlayer interaction, g_{12} , for two fixed values of the interlayer interaction, g_{11} , (upper and lower frames) presented for the planes (right frames) and chains (left frames) separately. In all frames the solid curve is the d -wave component of the order parameter, the short dashed curve is the extended s -wave component and the long dashed curve is the isotropic s -wave component. In the upper frames $g_{11} = 26.2$ and for $g_{12} = 10$, $T_c = 100K$. At $g_{12} = 0$ the order parameter is zero in the chains and is pure d -wave in the planes. As the interlayer interaction is increased the order parameter becomes present in the chains and there is a mixing of s -wave components. In the lower frames $g_{11} = 9.18$ and for $g_{12} = 20$, $T_c = 100K$. At $g_{12} = 0$ the order parameter is zero in both the chains and the planes. As the interlayer interaction is increased the order parameter becomes present in both the chains and planes and there is a mixing of s -wave components with the isotropic s -wave component eventually becoming dominant. The feature at $g_{12} \sim 25$ occurs when the gap node leaves the Brillouin zone. As discussed in the text there is a $g_{12} \leftrightarrow -g_{12}$ symmetry. Both g_{11} and g_{12} are in units of t_1 ; g_{22} , the coupling in the chains, is set equal to zero.

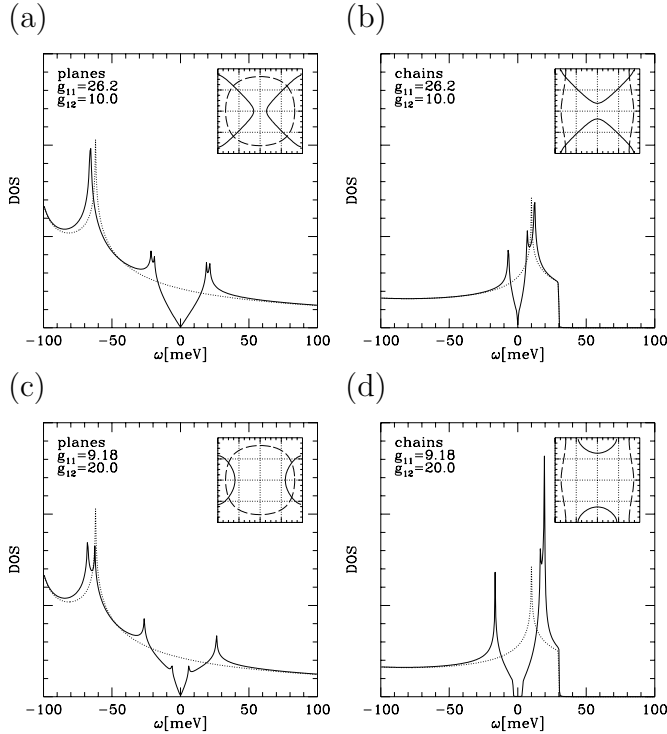


FIG. 3. Calculation of the superconducting (solid curves) and normal (dotted curves) density of states (DOS) for two sets of interaction parameters $g_{\alpha\beta}$ (upper and lower frames) presented separately for the planes (left frames) and chains (right frames). Some experiments are surface probes and may probe either the planes or chains independently. The insets show the Fermi surface (dashed curve) and gap nodes (solid curve) in the planes and chains for the two different parameter choices in the first Brillouin zone with (π, π) at the center. In the upper frames, (a) and (b), we have chosen $\{g_{11}, g_{12}, g_{22}\} = \{26.2, 10, 0\}$ which gives $T_c = 100K$. In the lower frames, (c) and (d), we have chosen $\{g_{11}, g_{12}, g_{22}\} = \{9.18, 20, 0\}$ which also gives $T_c = 100K$. Note that for the second parameter choice the gap nodes do not cross the Fermi surface in the chains (frame (d), inset) and that the DOS is gapped. The c -axis Josephson resistance-tunneling current product for a YBCO-Pb junction for a pure d -wave order parameter is zero due to the equal parts of the order parameter with opposite signs. Here this is not the case (insets) and the c -axis Josephson resistance-tunneling currents product for a YBCO-Pb junction are (a) $\pm 0.18\text{meV}$, (b) 2.35meV , (c) $\pm 0.25\text{meV}$, and (d) 2.17meV . The relative sign is due to the relative sign of the s -wave components of the order parameter (ie, the only part which contributes).

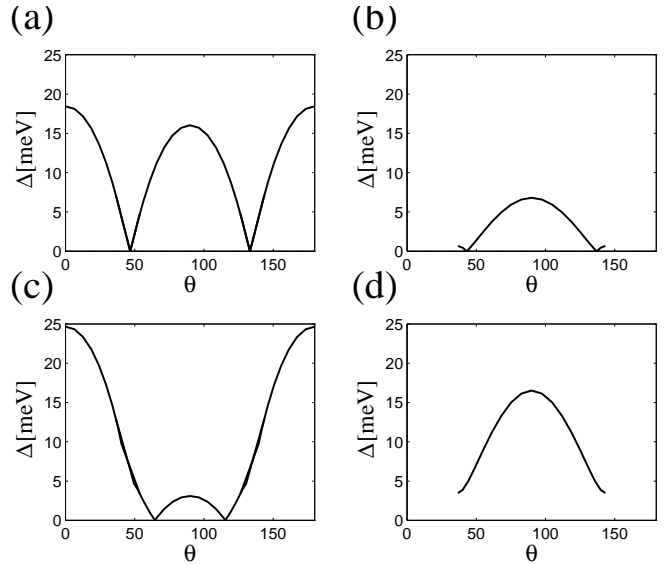


FIG. 4. The magnitude of the gap on the Fermi surface as a function of angle for the four cases of Figs. 2 and 3. The angle θ is measured from the center or (π, π) point of the Brillouin zone with the y -axis (ie, the vertical in the insets of Fig. 3) corresponding to $\theta = 0$. Frames (b) and (d) do not span all angles due to the Fermi surface not being closed in the chain layer. For the first choice of interaction parameters, $\{g_{11}, g_{12}, g_{22}\} = \{26.2, 10, 0\}$, the ratio $2\Delta_{\max(\text{FS})}/T_c$, where $\Delta_{\max(\text{FS})}$ is the maximum value of the gap on the Fermi surface, is 4.3 and 1.6 for the planes and chain respectively; for the second, $\{g_{11}, g_{12}, g_{22}\} = \{9.18, 20, 0\}$, they are 5.7 and 3.8.

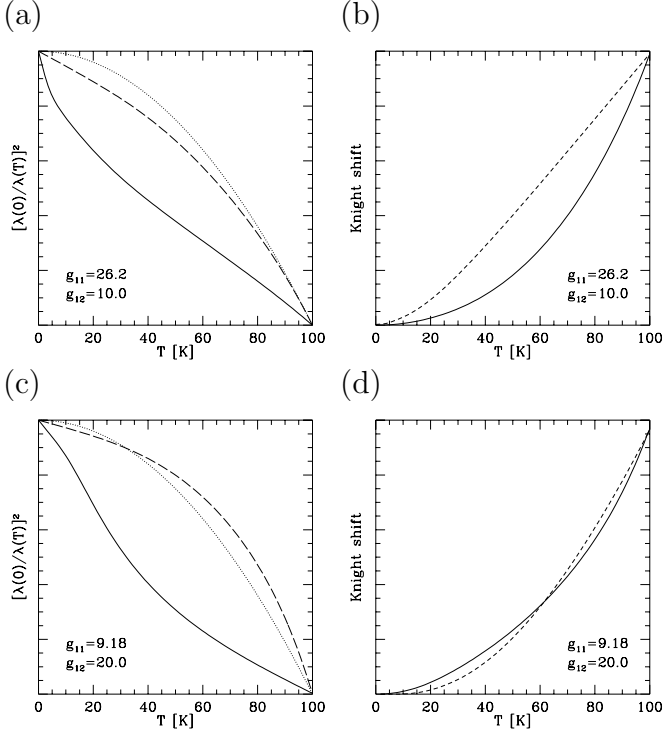


FIG. 5. Calculations of the magnetic penetration depth (left frames) and the Knight shift (right frames) for the two sets of interaction parameters. Frames (a) and (c) show the magnetic penetration depth along (solid curve) and perpendicular (dashed curve) to the CuO chains. The dotted curve is $1 - (T/T_c)^2$ and is shown for comparison. The chains, due to their Fermi surface, do not contribute appreciably to the penetration depth perpendicular to the chains (dashed curves). The ratio $(\lambda_{yy}/\lambda_{xx})^2$ is 1.37 for both sets of parameters since this is a normal state property. Frames (b) and (d) show the Knight shift in the planes (solid curves) and chains (dashed curves); due to the crossing of the gap nodes and the Fermi surface in the chains in (b) the Knight shift in the chain is a power law at low temperature, while due to the finite gap in (d) the Knight shift in the chain is exponential at low temperature.